Reactivity of the Tetrametallic Carbido Cluster $(C_5Me_5)WOs_3(\mu_4\text{-}C)(\mu\text{-}H)(CO)_{11}$ with Alkyne: Isomerization of an Allyl Fragment on a Tetrametallic Cluster Framework and Ring-Methyl Activation in the C_5Me_5 Ligand

Cathy Chung,[†] Wen-Cheng Tseng,[†] Yun Chi,*[,†] Shie-Ming Peng,*[,‡] and Gene-Hsiang Lee[‡]

Department of Chemistry, National Tsing Hua University, Hsinchu 30043, Taiwan, and Department of Chemistry and Instrumentation Center, National Taiwan University, Taipei 10764, Taiwan, Republic of China

Received December 4, 1997

Treatment of the tetrametallic carbido−benzofuryl cluster $(C_5Me_5)WOs_3(\mu_4\text{-}C)(\mu\text{-}H)_2(\mu\text{-}C_8H_6O)(CO)_9$ (**1**) with pressurized CO gas affords a carbido cluster $(C_5Me_5)WOs_3(\mu_4\text{-}C)(\mu\text{-}H)(CO)_{11}$ (**2**) in nearly quantitative yield. The reactions of **2** with diisopropyl acetylenedicarboxylate (DPAD) are investigated. If complex **2** is first treated with Me_3NO, the incorporation of DPAD at room temperature affords a cluster compound $(C_5Me_5)WOs_3(CO)_{10}[C_3H(CO_2Pr^i)_2]$ (**3**) in moderate yield, in which the allyl group is formed by hydride migration to the carbide. Complex **3** undergoes a facile metathesis to yield an isomer (**4**) with a different arrangement of the allyl C_3 backbone. Upon thermolysis, complex **4** converts to a η^6-tetramethylfulvene complex $[C_5Me_4(CH_2)]WOs_3(\mu\text{-}H)[C_3H(CO_2Pr^i)_2](CO)_9$ (**5**) by activation of a ring-methyl in the C_5Me_5 ligand and a trialkylidyne cluster $(C_5Me_5)WOs_3(\mu_3\text{-}CH)(\mu_3\text{-}CCO_2Pr^i)_2(CO)_9$ (**6**) by cleavage of two allyl C−C bonds. The possible mechanism of their interconversion is discussed. If the reaction of the Me_3NO-activated complex **2** and DPAD is carried out in refluxing toluene, we obtained one more compound $(C_5Me_5)WOs_3[CC_2(CO_2Pr^i)_2H](CO)_{10}$ (**7**) in low yield, which appears to form through a secondary process involving hydride migration to the DPAD molecule instead.

The chemistry of carbido cluster complexes has developed in recent years to constitute a distinct research domain.[1] For example, the early work of Bradley[2] and Shriver[3] on the reactivity of the Fe_4 system illustrated that the exposed carbide participated in the C−C and C−H bond formation by addition of methanol, alkylation reagents, or acids. In the related Ru_4 system, Lewis and Johnson reported the first coupling reaction involving carbide and diphenylacetylene.[4] These reactions are of noteworthy because they represent the key pathways for conversion of carbides to large hydrocarbon fragments on catalytic surfaces.[5] In a continuation of this type of investigation, our research group has discovered a reversible coupling between carbide and alkylidyne on metal cluster complexes,[6] a heretofore unidentified reaction, but has been extensively discussed according to the conformity between ligated acetylides and carbide−alkylidynes.[7] In this paper, we report a high-yield method of generating the target carbido cluster compound $(C_5Me_5)WOs_3(\mu_4\text{-}C)(\mu\text{-}H)(CO)_{11}$ (**2**) and the subsequent reactivity study of this carbido cluster with an electron-deficient alkyne.

In addition, one product $(C_5Me_5)WOs_3(CO)_{10}[C_3H(CO_2Pr^i)_2]$ (**3**) isolated from this coupling reaction, which contains a dimetallaallyl ligand, undergoes a series of rarely observed chemical transformations, involving cluster-assisted allyl metathesis, conversion of an η^5-C_5Me_5 to an η^6-tetramethylfulvene, and formation of three alkylidyne ligands by cleavage of two C−C bonds. Thus, the chemistry observed in the present study provides an ideal model to delineate various possible

[†] National Tsing Hua University.
[‡] National Taiwan University.

(1) (a) Bradley, J. S. *Adv. Organomet. Chem.* **1982**, *22*, 1. (b) Lewis, J.; Johnson, B. F. G. *Pure Appl. Chem.* **1982**, *54*, 97. (c) Johnson, B. F. G.; Lewis, J.; Nelson, W. J. H.; Nicholls, J. N.; Vargas, M. D. *J. Organomet. Chem.* **1983**, *249*, 255. (d) Jensen, M. P.; Henderson, W.; Johnston, D. H.; Sabat, M.; Shriver, D. F. *J. Organomet. Chem.* **1990**, *394*, 121. (e) *The Chemistry of Metal Cluster Complexes*; Shriver, D. F., Kaesz, H. D., Adams, R. D., Eds.; VCH: New York, 1990. (f) Karet, G. B.; Espe, R. L.; Stern, C. L.; Shriver, D. F. *Inorg. Chem.* **1992**, *31*, 2658. (g) Takahashi, Y.; Akita, M.; Moro-Oka, Y. *Chem. Commun.* **1997**, 1557.

(2) (a) Bradley, J. S.; Ansell, G. B.; Hill, E. W. *J. Am. Chem. Soc.* **1979**, *101*, 7417. (b) Bradley, J. S.; Hill, E. W.; Ansell, G. B.; Modrick, M. A. *Organometallics* **1982**, *1*, 1634.

(3) (a) Holt, E. M.; Whitmire, K. H.; Shriver, D. F. *J. Organomet. Chem.* **1981**, *213*, 125. (b) Holt, E. M.; Whitmire, K. H.; Shriver, D. F. *J. Am. Chem. Soc.* **1982**, *104*, 5621. (c) Wijeyesekera, S. D.; Hoffmann, R.; Wilker, C. N. *Organometallics* **1984**, *3*, 962. (d) Bogdan, P. L.; Woodcock, C.; Shriver, D. F. *Organometallics* **1987**, *6*, 1377.

(4) Dutton, T.; Johnson, B. F. G.; Lewis, J.; Owen, S. M.; Raithby, P. R. *J. Chem. Soc., Chem. Commun.* **1988**, 1423.

(5) (a) Tachikawa, M.; Muetterties, E. L. *J. Am. Chem. Soc.* **1980**, *102*, 4541. (b) Hriljac, J. A.; Swepston, P. N.; Shriver, D. F. *Organometallics* **1985**, *4*, 158.

(6) (a) Chiang, S.-J.; Chi, Y.; Su, P.-C.; Peng, S.-M.; Lee, G.-H. *J. Am. Chem. Soc.* **1994**, *116*, 11181. (b) Su, P.-C.; Chi, Y.; Su, C.-J.; Peng, S.-M.; Lee, G.-H. *Organometallics* **1997**, *16*, 1870.

(7) (a) Carty, A. J. *Pure Appl. Chem.* **1982**, *54*, 113. (b) Carty, A. J.; Taylor, N. J.; Sappa, E.; Tiripicchio, A.; Camellini, M. T. *Organometallics* **1991**, *10*, 1907. (c) Blenkiron, P.; Taylor, N. J.; Carty, A. J. *J. Chem. Soc., Chem. Commun.* **1995**, 327.

S0276-7333(97)01067-4 CCC: $15.00
Publication on Web 04/26/1998

reactions between carbide, hydride, and small unsaturated organic fragments and to interpret the novel reactivities for the allyl and the C_5Me_5 ligand of polynuclear cluster compounds.

Experimental Section

General Information and Materials. Infrared spectra were recorded on a Perkin-Elmer 2000 FT-IR spectrometer. ^1H and ^{13}C NMR spectra were recorded on a Bruker AM-400 (400.13 MHz) or a Bruker AMX-300 (300.6 MHz) instrument. Mass spectra were obtained on a JEOL-HX110 instrument operating in fast-atom bombardment modes (FAB). All reactions were performed under a nitrogen atmosphere using solvents dried with an appropriate reagent. The products were separated on commercially available preparative thin-layer chromatographic plates (Kieselgel 60 F_{254}, E. Merck). Elemental analyses were performed at the NSC Regional Instrumentation Center at National Cheng Kung University, Tainan, Taiwan.

Synthesis of $(C_5Me_5)WOs_3(\mu_4\text{-}C)(\mu\text{-}H)(CO)_{11}$. A toluene solution (75 mL) of $(C_5Me_5)WOs_3(\mu_4\text{-}C)(C_8H_5O)(\mu\text{-}H)_2(CO)_9$ (**1**, 1.6 g, 1.26 mmol) was placed in a 100 mL stainless steel Parr high-pressure reactor. Then the reactor was charged with 650 psi of CO gas, and the solution was stirred at 135 °C for 2 h. After the reactor was cooled to room temperature, the CO gas was released and the solvent was removed *in vacuo*. The orange residue was taken up in minimum amount of CH_2Cl_2 and recrystallized in a mixture of CH_2Cl_2 and methanol, giving 1.49 g of $(C_5Me_5)WOs_3(\mu_4\text{-}C)(\mu\text{-}H)(CO)_{11}$ (**2**, 1.23 mmol, 97%) as light orange crystalline materials.

Spectral data for **2**: MS (FAB, ^{192}Os, ^{184}W) *m/z* 1216(M^+). IR(C_6H_{12}): ν(CO) 2086 (s), 2057 (vs), 2043 (s), 2035 (s), 2009 (vs), 1987 (m, br), 1970 (vw), 1958 (m, br), 1930 (w, br), 1914 (vw, br), 1878 (w, br) cm^{-1}. ^1H NMR (400 MHz, $CDCl_3$, 293 K): δ 2.06 (s, 15H), −24.48 (s, 1H). ^{13}C NMR (100 MHz, $CDCl_3$, 293 K): CO δ 212.6 (2C, J_{WC} = 164 Hz), 178.8 (3C, br), 176.7 (2C), 174.1 (2C), 165.6 (2C); δ 340.3 (μ_4-C, J_{WC} = 104 Hz), 101.6 (C_5Me_5), 10.8 (5Me). Anal. Calcd for $C_{22}H_{16}O_{11}Os_3W$: C, 21.82; H, 1.33. Found: C, 21.61; H, 1.36.

Reaction of 2 with DPAD. An acetonitrile solution (30 mL) of freshly sublimed Me_3NO (11.1 mg, 0.148 mmol) was added dropwise to a mixture of CH_2Cl_2 (60 mL), acetonitrile (10 mL), and **2** (150 mg, 0.123 mmol). The addition of Me_3NO caused the color of the solution to change from light yellow to orange. Two hours later, the solvents were removed *in vacuo* and the mixture was redissolved into 80 mL of CH_2Cl_2. DPAD (73 mg, 0.37 mmol) was added to this CH_2Cl_2 solution, and the resulting solution was stirred at room temperature for 20 h, until the color of solution changed from orange to dark red. The reaction mixture was then concentrated and separated by thin-layer chromatography. Development with a 1:1 mixture of CH_2Cl_2 and hexane produced a major red band, which was extracted from silica gel to yield 98 mg of $(C_5Me_5)WOs_3[C_3H(CO_2Pr^i)_2](CO)_{10}$ (**3**, 0.071 mmol, 57%).

Spectral data for **3**: MS (FAB, ^{192}Os, ^{184}W) *m/z* 1386 (M^+). IR (C_6H_{12}): ν(CO) 2074 (s), 2008 (vs), 1999 (s), 1981 (m), 1965 (m), 1942 (m), 1844 (w, br) cm^{-1}. ^1H NMR (400 MHz, $CDCl_3$, 293 K): δ 7.97 (s, 1H), 5.04 (m, 2H, C*H*Me_2), 2.02 (s, 15H), 1.36 (d, J_{HH} = 6.2 Hz, 3H), 1.33 (d, J_{HH} = 6.3 Hz, 3H), 1.32 (d, J_{HH} = 6.2 Hz, 3H), 1.25 (d, J_{HH} = 6.2 Hz, 3H). ^{13}C NMR (100 MHz, CD_2Cl_2, 293 K): CO δ 230.8 (J_{WC} = 177 Hz), 218.1 (J_{WC} = 139 Hz), 194.8, 191.4, 186.0, 185.7 (br), 184.0, 182.5, 180.4, 178.6 (br), 174.0 (br), 170.7; δ 126.8, 119.9 (CH), 105.8 (C_5Me_5), 102.9, 75.2 (*C*HMe_2), 70.9 (*C*HMe_2), 22.3 (Me), 22.0 (2Me), 21.0 (Me), 10.3 (5Me). Anal. Calcd for $C_{31}H_{30}O_{14}Os_3W$: C, 26.96; H, 2.19. Found: C, 27.34; H, 2.32.

Thermolysis of 3. A toluene solution (50 mL) of **3** (50 mg, 0.036 mmol) was heated at 90 °C for 4 h, during which time the color changed from red to orange. The solvent was removed *in vacuo*, and the residue was taken up in minimum amount of CH_2Cl_2 and separated by thin-layer chromatography with a mixture of CH_2Cl_2 and hexane (4:1), giving 5 mg of $(C_5Me_5)WOs_3[C_3(CO_2Pr^i)_2H](CO)_{10}$ (**4**, 0.0036 mmol, 10%), 5 mg of $[C_5Me_4(CH_2)]WOs_3(\mu\text{-}H)[C_3H(CO_2Pr^i)_2](CO)_9$ (**5**, 0.0037 mmol, 10%), and 20 mg of $(C_5Me_5)WOs_3(\mu_3\text{-}CH)(\mu_3\text{-}CCO_2Pr^i)_2(CO)_9$ (**6**, 0.015 mmol, 41%).

Spectral data for **4**: MS (FAB, ^{192}Os, ^{184}W) *m/z* 1386 (M^+). IR (C_6H_{12}): ν(CO) 2077 (s), 2010 (vs), 1999 (s), 1966 (m), 1944 (m), 1830 (w, br) cm^{-1}. ^1H NMR (400 MHz, $CDCl_3$, 293 K): δ 8.72 (s, 1H), 5.07 (m, J_{HH} = 6.2 Hz, 1H, C*H*Me_2), 4.94 (m, J_{HH} = 6.3 Hz, 1H, C*H*Me_2), 2.02 (s, 15H), 1.39 (d, J_{HH} = 6.3 Hz, 3H), 1.30 (d, J_{HH} = 6.2 Hz, 3H), 1.28 (d, J_{HH} = 6.2 Hz, 3H), 1.26 (d, J_{HH} = 6.3 Hz, 3H). ^{13}C NMR (150 MHz, CD_2Cl_2, 293 K): CO δ 232.0 (J_{WC} = 176 Hz), 217.7 (J_{WC} = 138 Hz), 193.3, 189.8, 185.6 (br), 184.6, 183.4, 182.7, 179.1, 177.6 (br), 176.8, 173.2 (br); δ 130.7, 118.6 (CH), 105.7 (C_5Me_5), 96.9, 74.9 (*C*HMe_2), 69.7 (*C*HMe_2), 21.8 (Me), 21.7 (Me), 21.6 (Me), 21.1 (Me), 10.0 (5Me). Anal. Calcd for $C_{31}H_{30}O_{14}Os_3W$: C, 26.96; H, 2.19. Found: C, 27.37; H, 2.32.

Spectral data for **5**: MS (FAB, ^{192}Os, ^{184}W) *m/z* 1358 (M^+). IR (C_6H_{12}): ν(CO) 2087 (s), 2065 (vs), 2027 (vs), 2012 (s), 1996 (m), 1981 (w), 1972 (w), 1954 (m), 1840 (s), 1694 (m, br) cm^{-1}. ^1H NMR (400 MHz, $CDCl_3$, 293 K): δ 8.77 (s, 1H), 5.04 (m, 2H, C*H*Me_2), 3.85 (d, J_{HH} = 3.2 Hz, 1H), 3.36 (s, 3H), 2.27 (d, J_{HH} = 3.2 Hz, 1H), 2.05 (s, 3H), 1.61 (s, 3H), 1.37 (d, J_{HH} = 6.4 Hz, 3H), 1.32 (d, J_{HH} = 6.3 Hz, 6H), 1.29 (d, J_{HH} = 6.1 Hz, 3H), 0.80 (s, 3H), −20.28 (s, 1H). ^{13}C NMR (100 MHz, CD_2Cl_2, 293 K): CO δ 194.6, 185.2, 184.5, 183.1, 182.5, 176.6, 176.3, 175.8, 175.4, 168.2, 167.5; δ 133.8, 133.3, 128.1 (CH), 123.6 (C_5-ring), 117.6 (C_5-ring), 113.2 (C_5-ring), 99.2 (C_5-ring), 99.0 (C_5-ring), 70.5 (*C*HMe_2), 70.3 (*C*HMe_2), 56.8 (CH_2), 22.8 (Me), 22.5 (Me), 22.3 (2Me), 19.8 (Me), 13.4 (Me), 9.1 (Me), 8.8 (Me). Anal. Calcd for $C_{30}H_{30}O_{13}Os_3W$: C, 26.63; H, 2.23. Found: C, 27.19; H, 2.31.

Spectral data for **6**: MS (FAB, ^{192}Os, ^{184}W) *m/z* 1358 (M^+). IR (C_6H_{12}): ν(CO) 2089 (m), 2058 (vs), 2011 (m), 1997 (s), 1981 (m), 1971 (w), 1671 (vw) cm^{-1}. ^1H NMR (400 MHz, $CDCl_3$, 293 K): δ 8.37 (s, J_{WH} = 32 Hz, 1H), 5.02 (m, J_{HH} = 6.3 Hz, 2H), 2.04 (s, 15H), 1.34 (d, J_{HH} = 6.3 Hz, 12H).^{13}C NMR (100 MHz, CD_2Cl_2, 293 K): δ 182.7 (2*C*O_2Pr^i, J_{WC} = 26 Hz), 172.0 (br, 3CO), 171.3 (6C, CO), 157.5 (μ_3-CH, J_{WC} = 102 Hz), 156.1 (2C, μ_3-C, J_{WC} = 105 Hz), 109.0 (C_5Me_5), 69.8 (2*C*HMe_2), 22.0 (4Me), 10.4 (5Me). Anal. Calcd for $C_{30}H_{30}O_{13}Os_3W$: C, 26.63; H, 2.23. Found: C, 27.14; H, 2.30.

Reaction of 2 with DPAD, Second Method. An acetonitrile solution (30 mL) of freshly sublimed Me_3NO (23.5 mg, 0.33 mmol) was added dropwise to a mixture of CH_2Cl_2 (60 mL), acetonitrile (10 mL), and complex **2** (250 mg, 0.206 mmol) over a period of 2 h. The solvent was removed under vacuum, the mixture was redissolved into 75 mL of toluene. After the addition of DPAD (103 μL), the mixture was heated at 110 °C for 5 min. The solution was then removed under vacuum, and the residue was separated by thin-layer chromatography. Development with a 1:1 mixture of CH_2Cl_2 and hexane produced four bands, which were extracted from silica gel to yield 9 mg of **4** (0.006 mmol, 3%), 25 mg of **5** (0.018 mmol, 9%), 6 mg of **6** (0.004 mmol, 2%), and 15 mg of brown $(C_5Me_5)WOs_3[CC_2(CO_2Pr^i)_2H](CO)_{10}$ (**7**, 0.011 mmol, 5%).

Spectral data for **7**: MS (FAB, ^{192}Os, ^{184}W) *m/z* 1386 (M^+). IR (C_6H_{12}): ν(CO) 2076 (s), 2040 (s), 2018 (vs), 2003 (s), 1979 (m), 1965 (w), 1831 (w,br), 1718 (m) cm^{-1}. ^1H NMR (300 MHz, CD_2Cl_2, 293 K): δ 5.27 (m, J_{HH} = 6.2 Hz, 1H), 5.03 (m, J_{HH} = 6.2 Hz, 1H), 2.82 (s, 1H), 2.01 (s, 15H), 1.38 (d, J_{HH} = 6.2 Hz, 3H), 1.35 (d, J_{HH} = 6.2 Hz, 3H), 1.21 (d, J_{HH} = 6.2 Hz, 3H), 1.17 (d, J_{HH} = 6.2 Hz, 3H). ^{13}C NMR (75 MHz, CD_2Cl_2, 293 K): CO δ 216.7 (J_{WC} = 161 Hz), 216.5 (J_{WC} = 166 Hz), 184.8, 181.6 (3C), 181.0, 178.6 (3C), 172.5, 168.2; δ 285.7 (J_{WC} = 110 Hz), 110.0, 105.1 (C_5Me_5), 72.1 (*C*HMe_2), 69.4 (*C*HMe_2), 22.9 (CH), 22.3 (Me), 22.2 (Me), 22.1 (2Me), 11.3 (5Me). Anal. Calcd for $C_{31}H_{30}O_{14}Os_3W$: C, 26.96; H, 2.19. Found: C, 27.35; H, 2.23.

Table 1. X-ray Structural Data of Complexes 3−7[a]

compound	**3**	**4**	**5**	**6**	**7**
formula	$C_{31}H_{30}O_{14}Os_3W$	$C_{31}H_{30}O_{14}Os_3W$	$C_{30}H_{30}O_{13}Os_3W$	$C_{30}H_{30}O_{13}Os_3W$	$C_{31}H_{30}O_{14}Os_3W$
mol wt	1381.0	1381.01	1353.0	1353.0	1424.12
cryst syst	monoclinic	orthorhombic	triclinic	orthorhombic	triclinic
space group	$P2_{1/c}$	$Pca2_1$	$P\bar{1}$	$Pnma$	$P\bar{1}$
a (Å)	17.928(4)	19.789(4)	9.492(2)	19.272(4)	10.423(2)
b (Å)	20.112(3)	9.373(4)	12.216(2)	18.303(3)	18.606(3)
c (Å)	20.160(5)	19.068(3)	15.287(4)	9.565(3)	18.667(3)
α (deg)			80.27(2)		92.89(2)
β (deg)	90.72(3)		79.56(2)		90.25(2)
γ (deg)			84.79(2)		94.44(2)
volume (Å^3)	7269(3)	3537(2)	1714.9(7)	3374(1)	3605(1)
Z	8	4	2	4	4
D_c (g/cm^3)	2.524	2.594	2.618	2.664	2.545
F(000)	4998	2499	1220	2443	2499
2θ (max)	50.0	55.0	45.0	55.0	45
h, k, l ranges	−21 to 21, 0 to 23, 0 to 23	0 to 25, 0 to 12, 0 to 24	−10 to 10, 0 to 13, −15 to 16	0 to 25, 0 to 23, 0 to 12	−11 to 11, 0 to 20, −20 to 20
cryst size, mm	0.20 × 0.50 × 0.60	0.13 × 0.25 × 0.14	0.02 × 0.10 × 0.15	0.05 × 0.25 × 0.35	0.20 × 0.25 × 0.40
μ(Mo Kα), cm^{-1}	137.5	141.4	145.7	148.1	138.62
transmission; max, min	1.000, 0.245	1.000, 0.415	1.000, 0.479	1.000, 0.395	1.000, 0.629
no. of data in refinement	7114 with I ≥ 2σ(I)	3308 with I ≥ 2σ(I)	2893 with $I \geq 2\sigma(I)$	2603 with $I \geq 2\sigma(I)$	6389 with $I \geq 2\sigma(I)$
no. of atoms and params	158, 884	79, 442	76, 425	43, 224	158, 884
weight modifier, g	0.019	0.0001	0.0001	0.0001	0.0001
max Δ/σ ratio	0.002	0.031	0.0045	0.003	0.014
R_F; R_w	0.050; 0.042	0.039; 0.039	0.036; 0.034	0.038; 0.040	0.032; 0.030
GOF	1.46	1.49	1.21	1.48	1.19
D-map, max/min e/Å^3	3.52/−2.23	3.30/−1.93	1.38/−1.70	1.24/−1.59	0.91/−0.87

[a] Features common to all determinations: Nonius CAD-4 diffractometer, λ(Mo Kα) = 0.7107 Å. Minimized function: $\sum(w|F_o - F_c|^2)$. Weighting scheme: $w^{-1} = \sigma^2(F_o) + |g| F_o^2$; GOF = $[\sum w|F_o - F_c|^2/(N_o - N_v)]^{1/2}$ (N_o = number of observations; N_v = number of variables).

Table 2. Selected Bond Distances (Å) and Angles (deg) of 3[a]

W−Os(1)	2.906(1)	W−Os(2)	2.860(1)
Os(1)−Os(2)	2.802(1)	Os(1)−Os(3)	2.852(1)
Os(2)−Os(3)	2.773(1)	W−O(13)	2.20(1)
Os(1)−C(13)	2.13(2)	Os(2)−C(13)	2.23(2)
Os(2)−C(12)	2.30(2)	Os(2)−C(11)	2.25(2)
Os(3)−C(11)	2.14(2)	C(11)−C(12)	1.38(3)
C(12)−C(13)	1.42(2)	C(13)−C(18)	1.42(3)
C(18)−O(13)	1.24(2)		

∠W−O(13)−C(18)	120(1)	∠C(11)−C(12)-C(13)	120(2)
∠C(12)−C(13)-C(18)	121(2)	∠W−C(9)−O(9)	177(2)
∠W−C(10)−O(10)	164(2)		

[a] Esd in parentheses.

Table 3. Selected Bond Distances (Å) and Angles (deg) of 4[a]

W−Os(1)	2.863(1)	W−Os(3)	2.900(1)
Os(1)−Os(2)	2.768(1)	Os(1)−Os(3)	2.796(1)
Os(2)−Os(3)	2.850(1)	W−O(11)	2.21(1)
Os(1)−C(15)	2.22(2)	Os(3)−C(15)	2.11(2)
Os(1)−C(16)	2.33(2)	Os(1)−C(17)	2.30(2)
Os(2)−C(17)	2.07(2)	C(14)−C(15)	1.48(3)
C(15)−C(16)	1.40(3)	C(16)−C(17)	1.44(3)
C(14)−O(11)	1.24(2)		

∠W−O(11)−C(14)	117(1)	∠C(14)−C(15)-C(16)	114(2)
∠C(15)−C(16)-C(17)	118(2)	∠C(16)−C(17)-C(18)	113(2)
∠W−C(9)−O(9)	174(2)	∠W−C(10)−O(10)	165(2)

[a] Esd in parentheses.

Table 4. Selected Bond Distances (Å) and Angles (deg) of 5[a]

W−Os(1)	2.926(1)	W−Os(2)	2.676(1)
W−Os(3)	2.962(1)	Os(1)−Os(2)	2.865(1)
Os(1)−Os(3)	2.910(1)	Os(2)−Os(3)	2.852(1)
W−C(14)	2.16(2)	W−C(15)	2.33(2)
W−C(16)	2.22(2)	Os(1)−C(14)	2.18(2)
Os(3)−C(16)	2.14(2)	W−C(21)	2.34(2)
W−C(22)	2.17(2)	W−C(23)	2.30(2)
W−C(24)	2.48(2)	W−C(25)	2.53(2)
W−C(27)	2.32(2)		

∠C(13)−C(14)-C(15)	113(1)	∠C(14)−C(15)-C(16)	119(1)
∠C(15)−C(16)-C(17)	109(1)	∠W−C(22)−C(27)	77(1)

[a] Esd in parentheses.

X-ray Crystallography. The X-ray diffraction measurements were carried out on a Nonius CAD-4 diffractometer at room temperature. Lattice parameters were determined from 25 randomly selected high-angle reflections. Three standard reflections were monitored every 3600 s. No significant change in intensity (≤2%) was observed during the course of data collection. Intensities of the diffraction signals were corrected for Lorentz, polarization, and absorption effects (ψ scans). The structure was solved by using the NRCC-SDP-VAX package. All of the non-hydrogen atoms had anisotropic temperature factors, while the hydrogen atoms of the organic substituents were placed at the calculated positions with $U_H = U_C + 0.1$. The crystallographic refinement parameters of complexes **3**−**7** are given in Table 1, while their selected bond distances and angles are presented in Tables 2−6.

Results

Synthesis and Characterization of Carbido Cluster 2. The target carbido carbonyl complex $(C_5Me_5)WOs_3(\mu_4\text{-}C)(\mu\text{-}H)(CO)_{11}$ (**2**), which possesses a wingtip W atom, a multisite bound carbide, and a hydride spanning the Os−Os hinge, was obtained in nearly quantitative yield from treatment of butterfly carbido−benzofuryl cluster $(C_5Me_5)WOs_3(\mu_4\text{-}C)(\mu\text{-}H)_2(\mu\text{-}C_8H_6O)(CO)_9$ (**1**) with pressurized CO gas (50 atm, 135 °C, 2 h).[8] (Scheme 1) The identification of **2** was achieved by routine spectroscopic methods. Solution infrared spectroscopy shows that the pattern of the CO stretching peaks is similar to that of the structurally characterized carbido cluster complex $(C_5Me_5)WRu_3(\mu_4\text{-}C)(\mu\text{-}H)(CO)_{11}$.[9] The ^{1}H NMR spectrum exhibits the presence of a high-

(8) (a) Chi, Y.; Su, P.-C.; Peng, S.-M.; Lee, G.-H. *Organometallics* **1995**, *14*, 5483. (b) Chi, Y.; Chung, C.; Chou, Y.-C.; Su, P.-C.; Chiang, S.-J.; Peng, S.-M.; Lee, G.-H. *Organometallics* **1997**, *16*, 1702.

Table 5. Selected Bond Distances (Å) of 6[a]

W−Os(1)	2.835(1)	W−Os(2)	2.818(1)
Os(1)−Os(2)	3.008(1)	Os(2)···Os(2)	3.253(1)
W−C(6)	1.98(2)	Os(2)−C(6)	2.20(1)
W−C(7)	2.00(1)	Os(1)−C(7)	2.19(1)
Os(2)−C(7)	2.16(1)		

[a] Esd in parentheses.

Table 6. Selected Bond Distances (Å) and Angles (deg) of 7[a]

W−Os(1)	2.963(1)	W−Os(2)	2.975(1)
W−Os(3)	2.920(1)	Os(1)−Os(2)	2.745(1)
Os(1)−Os(3)	2.852(1)	Os(2)−Os(3)	2.819(1)
W−C(11)	2.08(1)	Os(1)−C(11)	2.03(1)
Os(3)−C(11)	2.04(1)	Os(1)−C(16)	2.16(2)
Os(1)−C(17)	2.25(1)	C(11)−C(16)	1.43(2)
C(16)−C(17)	1.42(2)		
∠W−C(9)−O(9)	162(1)	∠W−C(10)−O(10)	170(1)
∠Os−CO(mean)	177(1)	∠C(11)−C(16)-C(17)	116(1)

[a] Esd in parentheses.

Scheme 1

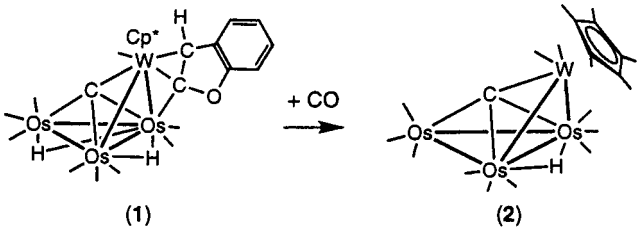

(1) (2)

field hydride signal at δ −24.48, together with the sharp signal at δ −2.06 due to the C_5Me_5 ligand. In addition, the ^{13}C NMR spectrum gives one W−CO signal at δ 212.6 (2C, J_{WC} = 164 Hz) and four Os−CO signals at δ 178.8 (3C, br), 176.7 (2C), 174.1 (2C), 165.6 (2C). The broad signal at δ 178.8 is assigned to the CO ligands of the unique $Os(CO)_3$ vertex at the wingtip position, while the observation of three more Os−CO signals with ratio of 2:2:2 is consistent with the formation of a time-averaged mirror plane which bisects the whole molecule. The final confirmation comes from the detection of a downfield signal at δ 340.3 with J_{WC} = 104 Hz, which unambiguously suggests the existence of the μ_4-carbide ligand.

Reaction of 2 with Alkyne. Complex **2** showed poor reactivity with diisopropyl acetylenedicarboxylate (DPAD) in toluene solution at reflux, and we only obtained the recovery of starting material under this condition. However, when the carbido cluster **2** was first treated with excess anhydrous Me_3NO in a mixed solution of CH_2Cl_2 and acetonitrile, the addition of DPAD gave a red product $(C_5Me_5)WOs_3(CO)_{10}[C_3H(CO_2Pr^i)_2]$ (**3**) in 57% yield (room temperature, 20 h). The stoichiometry of **3** was initially confirmed by FAB mass analysis, which exhibited a parent ion at *m*/*z* 1386, showing a formula of $C_{31}H_{30}O_{14}Os_3W$. In addition, disappearance of the hydride signal and occurrence of a sharp singlet at δ 7.97 in the ^1H NMR spectrum suggests the formation of a CH fragment, accompanying coordination of the DPAD molecule. The X-ray diffraction study was then carried out to reveal the molecular structure of this addition product.

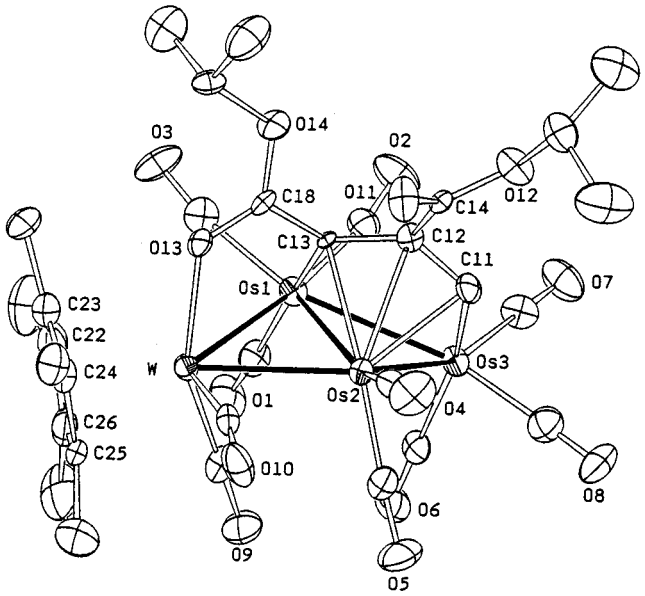

Figure 1. Molecular structure and atomic labeling scheme of the complex $(C_5Me_5)WOs_3(CO)_{10}[C_3H(CO_2Pr^i)_2]$ (**3**), with thermal ellipsoids shown at the 30% probability level.

Crystals of **3** contains two crystallographically distinct but structurally similar molecules in the asymmetric unit. A perspective view of one molecule is depicted in Figure 1, which consists of a butterfly arrangement of metal atoms and a dihedral angle of 153.85(4)°. The W atom is located at a wingtip position, while the other vertex is occupied by two $Os(CO)_3$ units and one $Os(CO)_2$ unit, the latter is located at a hinge site. The carbon atom C(11), which is derived from the carbido ligand of **2**, is now coupled with hydride and DPAD to form a dimetallaallyl fragment with two relatively short σ-bonds (Os(1)−C(13) = 2.13(2) Å and Os(3)−C(11) = 2.14(2) Å) and three slightly longer π-interactions (2.23(2)−2.30(2) Å) to the $Os(CO)_2$ group. Moreover, the carbonyl oxygen atom of one carboxylate fragment is coordinated to the W atom with a distance 2.20(1) Å, forming a ligand to metal dative bond in a manner similar to the complexes bearing carboxylate-substituted hydrocarbon ligands.[10] If we consider that this C═O→W interaction donates two electrons to the cluster core, then the molecule contains 62 valence electrons, which is typical for tetrametallic complexes with five metal−metal bonds.

The reactivity of **3** is of noteworthy. Thermolysis of **3** in toluene at 90 °C for 4 h afforded three complexes $(C_5Me_5)WOs_3(CO)_{10}[C_3(CO_2Pr^i)_2H]$ (**4**), $[C_5Me_4(CH_2)]WOs_3(\mu\text{-}H)[C_3H(CO_2Pr^i)_2](CO)_9$ (**5**), and $(C_5Me_5)WOs_3(\mu_3\text{-}CH)(\mu_3\text{-}CCO_2Pr^i)_2(CO)_9$ (**6**) in 10%, 10%, and 41% yields, respectively (Scheme 2). The time sequence of their formation is obtained by monitoring their individual reactivity. These investigations include heating a toluene solution of **4** at reflux for 2 h, which afforded a mixture **5** and **6** in 11% and 65% yields, while heating **5** under analogous conditions gave only **6** in 28% yield. Thus, these results clearly suggest that **4** is the kinetic product while **6** is the most stable, thermodynamic

(9) Chi, Y.; Chuang, S.-H.; Chen, B.-F.; Peng, S.-M.; Lee, G.-H. *J. Chem. Soc., Dalton Trans.* **1990**, 3033.

(10) (a) Adams, R. D.; Huang, M. *Organometallics* **1996**, *15*, 4437. (b) Adams, R. D.; Huang, M.; Zhang, L. *J. Cluster Sci.* **1997**, *8*, 101. (c) Chi, Y.; Wu, H.-L.; Peng, S.-M.; Lee, G.-H. *J. Chem. Soc., Dalton Trans.* **1997**, 1931.

Scheme 2

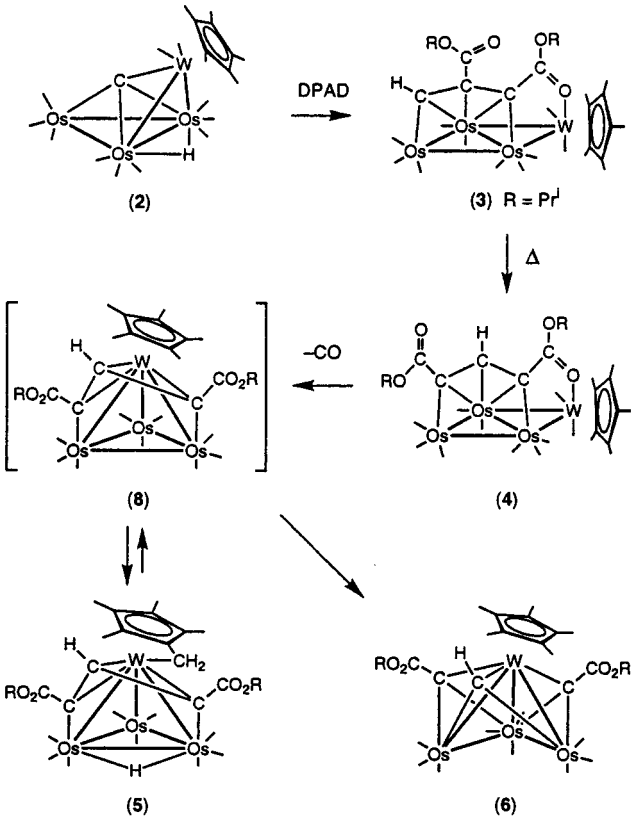

product of these thermally induced isomerization reactions.

The characterization of **4** is first provided by the IR ν(CO) spectrum. In solution, complex **4** gives a CO stretching pattern identical to that of **3**, suggesting that it is a structural isomer of **3**. Furthermore, the ^{13}C NMR spectrum exhibits a very similar spectral pattern for the allyl fragment and CO ligands, while the ^1H NMR spectrum shows a CH signal shifting to a downfield position at δ 8.72. On the basis of these observations, a structure with the CH fragment located at the middle of dimetallaallyl fragment is envisaged. In fact, a single-crystal X-ray diffraction study confirmed this proposal. As can be seen from the ORTEP diagram shown in Figure 2 and the selected distances listed in Table 3, the overall molecular geometry of **4**, which comprises the nearly planar WOs_3 framework and the expected allyl fragment, CRCHCR (R = CO_2Pr^i), with one carbonyl oxygen atom coordinated to the $(C_5Me_5)W(CO)_2$ fragment, is essentially identical to that of complex **3** discussed earlier.

For complex **5**, the ^1H NMR spectrum shows the expected CH grouping and two isopropyl signals for the allyl fragment CRCHCR, R = CO_2Pr^i. However, the sharp signal of the C_5Me_5 ligand is now replaced by four methyl signals at δ 3.36, 2.05, 1.61, and 0.80, two doublets at δ 3.85 and 2.27 (J_{HH} = 3.2 Hz) due to an exocyclic CH_2 group, and a hydride signal at δ −20.28. Such a dramatic change of the ^1H NMR spectral pattern strongly suggests that one methyl group of the C_5Me_5 ligand has undergone a C−H activation reaction to produce one hydride, one methylene, and four inequivalent methyl functional groups, giving the formation of tetramethylfulvene group. Accordingly, the ^{13}C NMR

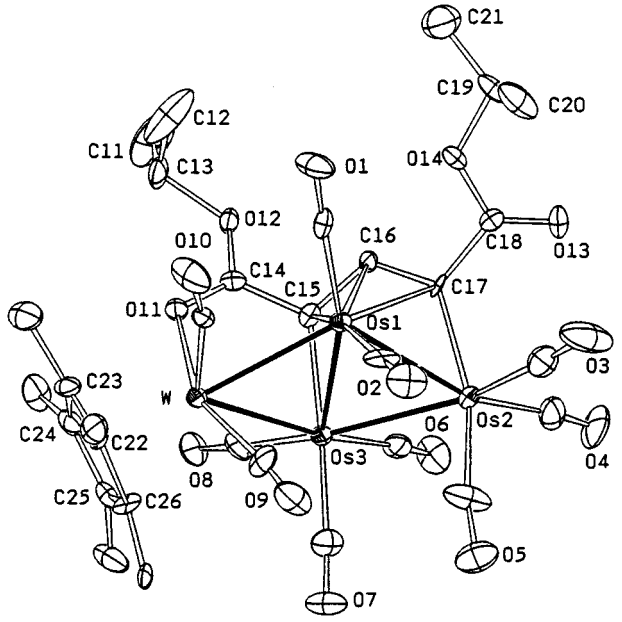

Figure 2. Molecular structure and atom labeling scheme of the complex $(C_5Me_5)WOs_3(CO)_{10}[C_3(CO_2Pr^i)_2H]$ (**4**), with thermal ellipsoids shown at the 30% probability level.

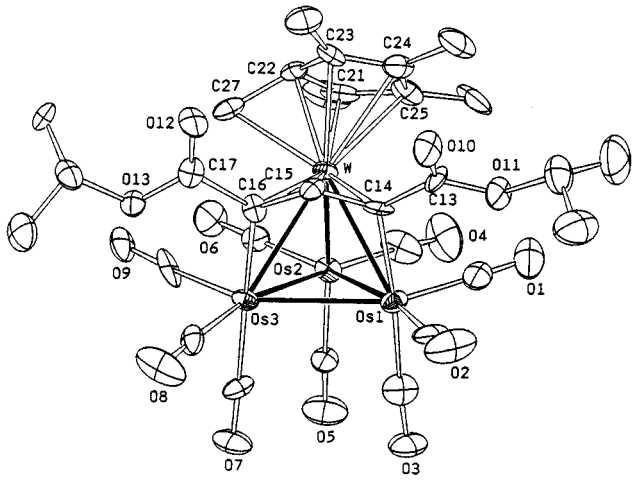

Figure 3. Molecular structure and atomic labeling scheme of the complex $[C_5Me_4(CH_2)]WOs_3(\mu\text{-}H)[C_3(CO_2Pri)_2H](CO)_9$ (**5**), with thermal ellipsoids shown at the 30% probability level.

spectrum exhibits five signals in the range δ 123.6−99.0, which are assigned to the five inner carbon atoms derived from the C_5Me_5 ligand, one methylene carbon signal at δ 56.8, and three more methyl signals at δ 22.8, 22.5, and 22.3 with a ratio of 1:1:2. Thus, the single-crystal X-ray diffraction analysis was carried out to confirm the bonding of this tetramethylfulvene group.

As indicated in Figure 3, the metal framework adopts a tetrahedral geometry with the W−Os(2) edge (2.676(1) Å) being the shortest within the molecule. In addition, the methylene carbon atom C(27) is coordinated to the W metal atom. The disposition of the C_5 ring and the exocyclic CH_2 arm is related to that found for the monometallic η^6-tetramethylfulvene complexes reported.[11] Other important features involve the allyl group μ_3-CRCHCR, R = CO_2Pr^i, which is coordinated to a WOs_2 metal triangle and possesses two CO_2Pr^i substituents at both terminal positions. The hydride ligand, although not located on the electron density

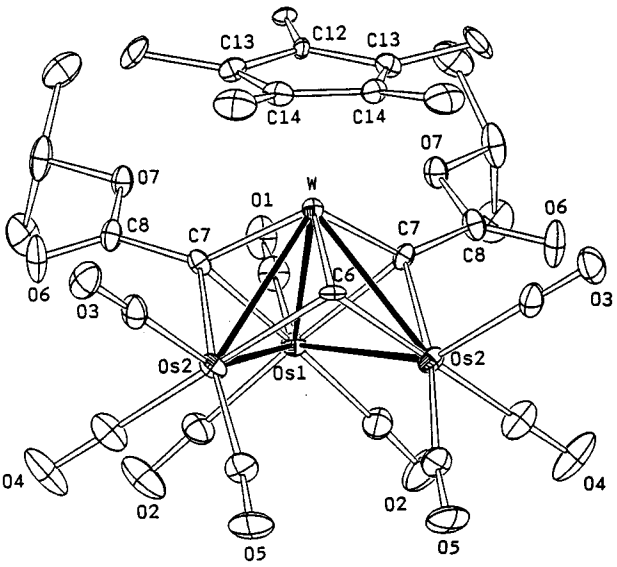

Figure 4. Molecular structure and atom labeling scheme of the complex $(C_5Me_5)WOs_3(\mu_3\text{-}CH)(\mu_3\text{-}CCO_2Pr^i)_2(CO)_9$ (**6**), with thermal ellipsoids shown at the 30% probability level.

map, is believed to associate with the Os−Os vector below the allyl ligand, as the corresponding Os(1)−Os(3) distance (2.910(1) Å) is significantly longer that the other Os−Os distances, Os(1)−Os(2) = 2.865(1) Å and Os(2)−Os(3) = 2.852(1) Å, of the tetrahedral cluster skeleton.

On the other hand, the ^{13}C NMR spectrum of **6** shows two alkylidyne C_α signals at δ 157.5 (J_{WC} = 102 Hz) and 156.1 (J_{WC} = 105 Hz) in a ratio of 1:2, although the observed chemical shifts are moved to the high-field region with respect to that reported for the μ_3-alkylidyne ligand.[12] The result of the X-ray diffraction study, which is in accordance with the ^{13}C NMR data, reveals a butterfly framework with a dihedral angle of 100.33(2)°, the existence of three alkylidyne ligands, and a crystallographical imposed mirror plane, passing the W−Os(1) hinge and bisecting the molecule (Figure 4). The Os(2)−Os(2) distance (3.253(1) Å) is fully compatible with the prediction based on the cluster valence-electron counting (62 electrons). The equivalent alkylidyne fragments, each carries a CO_2Pr^i fragment, are located at the outer face of each WOs_2 wing. The unique methylidyne ligand, which lies on the mirror plane, spans the hinge W atom and the wingtip Os atoms. Thus, the observed structure is related to that of the trialkylidyne complex $CpWOs_3(\mu_3\text{-}CTol)_3(CO)_9$ prepared by Park and co-workers.[13] Interestingly, the W−C_α distances (W−C(6) = 1.98(2) Å and W−C(7) = 2.00(1) Å) of the alkylidyne ligands are equal within the experimental errors. Thus, it suggests that the steric interaction between the C_5Me_5 ligand and the CO_2Pr^i substituent is about the same as that to the methylidyne hydrogen atom.

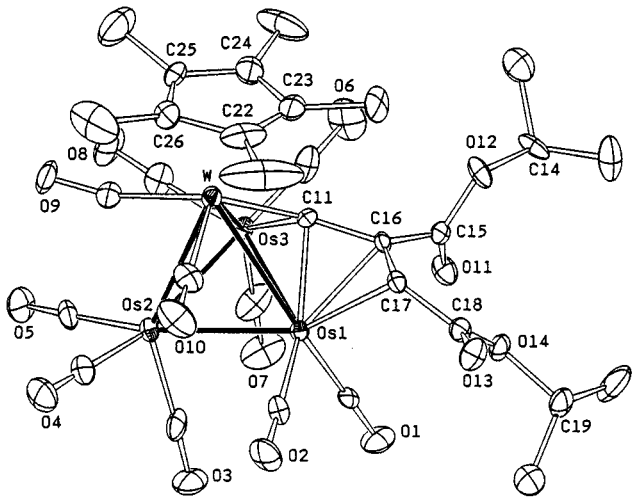

Figure 5. Molecular structure and atom labeling scheme of the complex $(C_5Me_5)WOs_3[CC_2(CO_2Pr^i)_2H](CO)_{10}$ (**7**), with thermal ellipsoids shown at the 30% probability level.

Chart 1

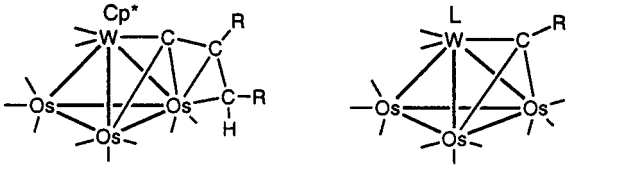

(7) R = CO_2Pr^i L = Cp, C_5Me_5; R = H, Me, Ph

Generation of a Vinyl Alkylidyne Cluster. To explore the other less probable reaction route occurring between the carbide and alkyne, we examined the reaction of the acetonitrile-substituted complex **2** with DPAD in refluxing toluene solution. It is noteworthy that in addition to the previously mentioned complexes **4**, **5**, and **6**, we isolated one more cluster complex $(C_5Me_5)WOs_3[CC_2(CO_2Pr^i)_2H](CO)_{10}$ (**7**) in low yield, Chart 1. This newly isolated complex shows a parent molecular ion at *m*/*z* 1386, which is identical to that of the allyl complexes **3** and **4**, suggesting the retention of the $WOs_3(CO)_{10}$ framework and the incorporation of one DPAD unit. The ^1H NMR spectrum of **7** exhibits the expected signals for the C_5Me_5 and two isopropyl groups and a sharp signal at δ 2.82 attributable to the CH proton. This ^1H NMR data is in accordance with the hydride migration to either the carbide atom or the DPAD fragment. Furthermore, the ^{13}C NMR spectrum exhibits two W-bound CO ligands at δ 216.7 (J_{WC} = 161 Hz) and 216.5 (J_{WC} = 166 Hz) and a downfield quaternary carbon signal at δ 285.7 with J_{WC} = 110 Hz, which is believed to be due to the α-carbon of a substituted alkylidyne functional group. In addition, this carbon atom is probably linked to the DPAD molecule but not the hydride ligand, as observed in **3**, because it gave no J_{CH} coupling. Therefore, these NMR spectral data implicate the formation of a different hydrocarbon ligand for **7**, and the single-crystal X-ray crystal structural analysis was examined to establish its identity.

As indicated in Figure 5, the cluster core consists of a tetrahedral geometry composed by two $Os(CO)_3$, one $Os(CO)_2$, and one $W(CO)_2$ metal vertex. The W−Os distances are about equal (2.920(1)−2.963(1) Å), while the Os(1)−Os(2) distance (2.745(1) Å) is slightly shorter

(11) (a) Schock, L. E.; Brock, C. P.; Marks, T. J. *Organometallics* **1987**, *6*, 232. (b) Yanovsky, A. I.; Struchkov, Y. T.; Kreindlin, A. Z.; Rybinskaya, M. I. *J. Organomet. Chem.* **1989**, *369*, 125. (c) Klahn, A. H.; Moore, M. H.; Perutz, R. N. *J. Chem. Soc., Chem. Commun.* **1992**, 1699. (d) Fan, L.; Turner, M. L.; Hursthouse, M. B.; Malik, K. M. A.; Gusev, O. V.; Maitlis, P. M. *J. Am. Chem. Soc.* **1994**, *116*, 385. (e) O'Leary, S. R.; Adams, H.; Maitlis, P. M. *Chem. Commun.* **1997**, 895.

(12) Evans, J.; McNulty, S. C. *J. Chem. Soc., Dalton Trans.* **1984**, 79.

(13) Park, J. T.; Woo, B. W.; Chung, J.-H.; Shim, S. C.; Lee, J.-H.; Lim, S.-S.; Suh, I.-H. *Organometallics* **1994**, *13*, 3384.

Scheme 3

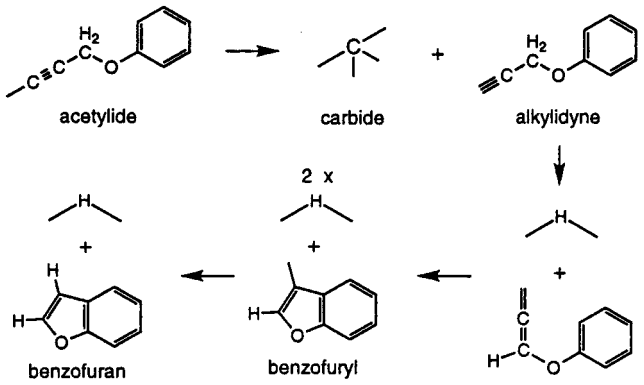

Scheme 4

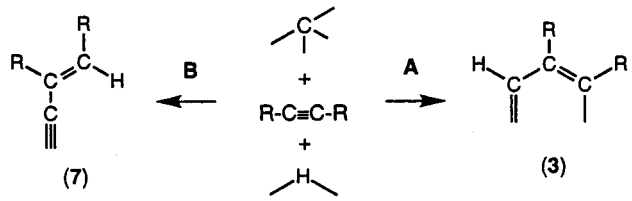

Chart 2

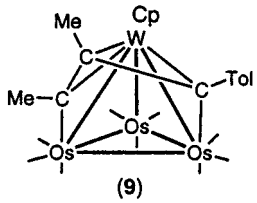

(9)

then the other two Os−Os distances (2.819(1) and 2.852(1) Å). The variation of the metal−metal distances is normal and falls within the expected range for the 60-electron, saturated WOs_3 cluster compound. The alkylidyne carbon atom C(11), which is obviously derived from the carbide ligand of **2**, resides on the W−Os(1)−Os(3) metal triangle and is linked to a vinyl fragment C(16)−C(17) with two CO_2Pr^i substituents located at the *cis*-position. This vinyl group, produced by the coupling of DPAD and the hydride, is further coordinated to the unique $Os(CO)_2$ vertex with slightly elongated bond lengths (Os(1)−C(16) = 2.16(2) Å and Os(1)−C(17) = 2.25(1) Å). If we ignored this secondary olefinic π-interaction, the overall molecular geometry is analogous to that of the structurally characterized alkylidyne compounds $LWOs_3(\mu_3\text{-}CR)(CO)_{11}$ (L = Cp and C_5Me_5; R = Tol and H),[14] which all possess a normal face-bridging alkylidyne ligand and three $Os(CO)_3$ metal vertexes at the basal positions of the cluster.

Discussion

We have developed a convenient and high-yield preparative route to the carbido cluster **2** from carbido−benzofuryl cluster **1**, a product which is initially prepared from acetylide complexes $(C_5Me_5)WOs_3(CCCH_2OPh)(CO)_{11}$. If we take this into consideration, the formation of **2** goes through the novel acetylide C−C bond cleavage to afford a carbide and alkylidyne (Scheme 3). The alkylidyne then isomerizes to give a benzofuryl substituent through a complex isomerization process involving sequential C−H bond activation, orthometalation, and C−C bond formation. Eventually, the removal of the benzofuryl substituent (probably as benzofuran) from the WOs_3 frame is effected by treatment with CO under pressure. This extraordinary reaction is parallel to the CO disproportionation reaction that has been widely applied for the synthesis of many group 8 carbido carbonyl clusters.[15]

The reactivity of **2** with an electron-deficient alkyne, DPAD, was then examined. It appears that the addition of Me_3NO is essential to lower the reaction barrier and to provide a potential coordination site for the incoming DPAD. For the reaction carried out at room temperature, we isolated the allyl cluster **3** as the major product, suggesting that the hydride migration to the carbide is an important key step (pathway A of Scheme 4). The hydride migration to the carbide atom has been observed in the related carbido complex $Ru_4(\mu_4\text{-}C)(\mu\text{-}H)_2(CO)_{12}$, in which the reversible hydride migration between the Ru−Ru and Ru−C(carbide) edges has been confirmed by a variable-temperature ^1H NMR study.[16] The resulting methylidyne ligand then reacts with the DPAD to afford the allyl ligand observed in **3**, for which the reaction is akin to those documented for other alkylidyne clusters and many alkynes.[17] Unfortunately, a simultaneous coupling of carbide, hydride, and DPAD or other possibilities cannot be satisfactorily ruled out at present.

Furthermore, if the reaction was executed in refluxing toluene, one additional cluster product **7** was isolated in lower yield. This result suggests the occurrence of a second, less favorable pathway which involves the hydride migration to the coordinated DPAD instead (pathway B of Scheme 4). Again, the timing of the C−C bond formation between the carbide and DPAD molecule in **7**, with respect to the hydride migration to DPAD, is uncertain based on our present experimental evidences.

The isolation of the allyl complex **3** provides a good opportunity to examine several important cluster reactions involving (i) allyl metathesis, (ii) cluster core rearrangement, and (iii) competitive C−H or C−C bond activation (Scheme 2). The conversion from complex **3** to its isomer **4** is best understood by cleavage of the allyl the C−C bond to give transient alkyne and alkylidyne fragments, followed by alkyne rotation and regeneration of the C−C bond. We believe that the latent unsaturation required for the C−C bond cleavage is provided by lifting the weak C═O→W dative interaction of the CO_2Pr^i substituent, as this isomerization proceeded with no loss of CO ligand and because the reaction is not affected

(14) (a) Busetto, J.; Green, M.; Hessner, B.; Howard, J. A. K.; Jeffery, J. C.; Stone, F. G. A. *J. Chem. Soc., Dalton Trans.* **1983**, 519. (b) Gong, J.-H.; Chen, C.-C.; Chi, Y.; Wang, S.-L.; Liao, F.-L. *J. Chem. Soc., Dalton Trans.* **1993**, 1829. (c) Gong, J.-H.; Hwang, D.-K.; Tsay, C.-W.; Chi, Y.; Peng, S.-M.; Lee, G.-H. *Organometallics* **1994**, *13*, 1720.

(15) (a) Hayward, C.-M. T.; Shapley, J. R. *Inorg. Chem.* **1982**, *21*, 3816. (b) Johnson, B. F. G.; Lewis, J.; Nicholls, J. N.; Puga, J.; Raithby, P. R.; Rosales, M. J.; McPartin, M.; Clegg, W. *J. Chem. Soc., Dalton Trans.* **1983**, 277. (c) Bailey, P. J.; Johnson, B. F. G.; Lewis, J. *Inorg. Chim. Acta* **1994**, *227*, 197.

(16) Cowie, A. G.; Johnson, B. F. G.; Lewis, J.; Raithby, P. R. *J. Organomet. Chem.* **1986**, *306*, C63.

(17) (a) Alami, M. K.; Dahan, F.; Mathieu, R. *Organometallics* **1985**, *4*, 2122. (b) Beanan, L. R.; Keister, J. B. *Organometallics* **1985**, *4*, 1713. (c) Churchill, M. R.; Ziller, J. W.; Shapley, J. R.; Yeh, W.-Y. *J. Organomet. Chem.* **1988**, *353*, 103. (d) Lentz, D.; Michael-Schulz, H. *Inorg. Chem.* **1990**, *29*, 4396. (e) Wong, W.-Y.; Chan, S.; Wong, W.-T. *J. Chem. Soc., Dalton Trans.* **1995**, 1497.

by exposing it to a CO atmosphere. The driving force of the isomerization is also deduced, which is believed to be the steric repulsion between the CO_2Pr^i substituents of the allyl ligand, as these functional groups are further away from each other in **4** and heating of a solution of **4** produces no detectable amount of the more congested precursor **3**.

Moreover, extensive heating of the allyl complex **4** in refluxing toluene solution led to the formation of a mixture of **5** and **6** (Scheme 2). Their formation can be visualized by, first, generation of an unsaturated, tetrahedral allyl intermediate complex (**8**) through removal of one CO ligand from the W atom. This hypothesis is further supported by the isolation of a structurally characterized, highly reactive Cp compound, $CpWOs_3(C_3Me_2Tol)CO)_9$ (**9**) Chart 2, which contains only 58 cluster valence electrons.[18] We believe that the unsaturated nature of **8** would induce the C−H activation at a methyl group of the nearby C_5Me_5 ligand, giving the formation of tetramethylfulvene and a bridging hydride, as observed in **5**. On the other hand, the same unsaturated cluster core would also promote the cleavage of allyl C−C bonds, affording the observed butterfly cluster **6**, which possesses three triply bridging alkylidyne ligands. Interestingly, the C−H bond activation of the methyl group is partially reversible as thermolysis of **5** gives the production of **6** in low yield. This conversion is best understood in terms of the regeneration of the intermediate **8**, which is then converted to complex **6** via the allyl C−C bond cleavage reaction discussed earlier.

(18) Kuo, M.-T.; Hwang, D.-K.; Liu, C.-S.; Chi, Y.; Peng, S.-M.; Lee, G.-H. *Organometallics* **1994**, *13*, 2142.

Summary

In summary, our studies provide a further example for the possible formation of a C−C bond between the carbide and alkyne and have shown that the cluster complexes formed can undergo facile conversion involving allyl metathesis, C−C bond cleavage, and other parallel processes such as C−H bond activation of a ring methyl in the C_5Me_5 ligand. The key intermediate is the tetrahedral complex **6**, which possesses an unsaturated cluster core with only 58 cluster valence electrons. A related investigation on the addition of alkenes to the carbido cluster **2**, which also shows the formation of a similar intermediate, will be described in the future.

Acknowledgment. We are grateful to the National Science Council of the Republic of China for financial support (Grant No. NSC 87-2113-M007-047).

Supporting Information Available: X-ray structural data including tables of bond distances, atomic coordinates, and thermal parameters for complexes **3**−**7** (32 pages). Ordering information is given on any current masthead page.

OM9710677